REPORT DOCUMENTATION PAGE

Form Approved OMB NO. 0704-0188

1. REPORT DATE (DD-MM-YYYY)	2. REPORT TYPE	3. DATES COVERED (From - To)
30-06-2013	Final Report	1-Jul-2012 - 31-Mar-2013

4. TITLE AND SUBTITLE

Final Report: Closing the Loop: Integrating Body, Muscle and Environment with Locomotion Central Pattern Generators

5a. CONTRACT NUMBER

W911NF-12-1-0264

5b. GRANT NUMBER

5c. PROGRAM ELEMENT NUMBER

611102

6. AUTHORS

Tim Kiemel, Kathleen Hoffman

5d. PROJECT NUMBER

5e. TASK NUMBER

5f. WORK UNIT NUMBER

7. PERFORMING ORGANIZATION NAMES AND ADDRESSES

University of Maryland - College Park
Research Administration
3112 Lee Building
College Park, MD 20742 -5141

8. PERFORMING ORGANIZATION REPORT NUMBER

9. SPONSORING/MONITORING AGENCY NAME(S) AND ADDRESS(ES)

U.S. Army Research Office
P.O. Box 12211
Research Triangle Park, NC 27709-2211

10. SPONSOR/MONITOR'S ACRONYM(S)

ARO

11. SPONSOR/MONITOR'S REPORT NUMBER(S)

61871-EG-II.1

12. DISTRIBUTION AVAILIBILITY STATEMENT

Approved for Public Release; Distribution Unlimited

13. SUPPLEMENTARY NOTES

The views, opinions and/or findings contained in this report are those of the author(s) and should not contrued as an official Department of the Army position, policy or decision, unless so designated by other documentation.

14. ABSTRACT

The role of sensory feedback is a central question in understanding vertebrate locomotion. Sensory feedback related to movement of the body and its interaction with the environment is known to have profound effects on the central pattern generator (CPG), the neural circuit responsible for generating the basic locomotor pattern. Conversely, the CPG controls muscle activation, leading to changes in body configurations as it interacts with the environment. We take two approaches to understanding the role of sensory feedback in locomotion: a

15. SUBJECT TERMS

optimal feedback control, central pattern generator, lamprey, locomotion, neural control

16. SECURITY CLASSIFICATION OF:			17. LIMITATION OF ABSTRACT	15. NUMBER OF PAGES	19a. NAME OF RESPONSIBLE PERSON
a. REPORT	b. ABSTRACT	c. THIS PAGE			Timothy Kiemel
UU	UU	UU	UU		19b. TELEPHONE NUMBER: 301-405-2488

Report Title

Final Report: Closing the Loop: Integrating Body,
Muscle and Environment with Locomotion Central Pattern Generators

ABSTRACT

The role of sensory feedback is a central question in understanding vertebrate locomotion. Sensory feedback related to movement of the body and its interaction with the environment is known to have profound effects on the central pattern generator (CPG), the neural circuit responsible for generating the basic locomotor pattern. Conversely, the CPG controls muscle activation, leading to changes in body configurations as it interacts with the environment. We take two approaches to understanding the role of sensory feedback in locomotion: a control-theory approach and a CPG-based approach. In the control theory approach, we have developed a general method of computing the optimal local feedback control law given a model of the plant (the mapping from muscle activation to movement) and a cost rate function that penalizes muscle activation and rewards speed through the environment. The first step in this method is to the compute the optimal steady-state swimming pattern. In the CPG-based approach, we have investigated the role of sensory feedback in a simple closed-loop model in which a CPG produces a pattern of muscle activation which is modified by sensory feedback related to body curvature.

Enter List of papers submitted or published that acknowledge ARO support from the start of the project to the date of this printing. List the papers, including journal references, in the following categories:

(a) Papers published in peer-reviewed journals (N/A for none)

Received Paper

TOTAL:

Number of Papers published in peer-reviewed journals:

(b) Papers published in non-peer-reviewed journals (N/A for none)

Received Paper

TOTAL:

Number of Papers published in non peer-reviewed journals:

(c) Presentations

Kiemel T, Hoffman K. Optimal open- and closed-loop control of anguilliform swimming. Oral presentation at the SIAM Conference on Applications of Dynamical Systems. May 19-23, 2013, Snowbird, UT, USA.

Number of Presentations: 1.00

Non Peer-Reviewed Conference Proceeding publications (other than abstracts):

Received Paper

TOTAL:

Number of Non Peer-Reviewed Conference Proceeding publications (other than abstracts):

Peer-Reviewed Conference Proceeding publications (other than abstracts):

Received Paper

TOTAL:

Number of Peer-Reviewed Conference Proceeding publications (other than abstracts):

(d) Manuscripts

Received Paper

TOTAL:

Number of Manuscripts:

Books

Received Paper

TOTAL:

Patents Submitted

Patents Awarded

Awards

NA

Graduate Students

NAME	PERCENT_SUPPORTED
FTE Equivalent:	
Total Number:	

Names of Post Doctorates

NAME	PERCENT_SUPPORTED
FTE Equivalent:	
Total Number:	

Names of Faculty Supported

NAME	PERCENT_SUPPORTED	National Academy Member
Tim Kiemel	0.39	
Kathleen Hoffman	0.22	
FTE Equivalent:	**0.61**	
Total Number:	**2**	

Names of Under Graduate students supported

NAME	PERCENT_SUPPORTED
FTE Equivalent:	
Total Number:	

Student Metrics

This section only applies to graduating undergraduates supported by this agreement in this reporting period

The number of undergraduates funded by this agreement who graduated during this period:	0.00
The number of undergraduates funded by this agreement who graduated during this period with a degree in science, mathematics, engineering, or technology fields:.....	0.00
The number of undergraduates funded by your agreement who graduated during this period and will continue to pursue a graduate or Ph.D. degree in science, mathematics, engineering, or technology fields:.....	0.00
Number of graduating undergraduates who achieved a 3.5 GPA to 4.0 (4.0 max scale):	0.00
Number of graduating undergraduates funded by a DoD funded Center of Excellence grant for Education, Research and Engineering:	0.00
The number of undergraduates funded by your agreement who graduated during this period and intend to work for the Department of Defense	0.00
The number of undergraduates funded by your agreement who graduated during this period and will receive scholarships or fellowships for further studies in science, mathematics, engineering or technology fields:	0.00

Names of Personnel receiving masters degrees

NAME

Total Number:

Names of personnel receiving PHDs

NAME

Total Number:

Names of other research staff

NAME PERCENT_SUPPORTED

FTE Equivalent:

Total Number:

Sub Contractors (DD882)

1 a. University of Maryland Baltimore County

1 b. Senior Grants and Contracts Manager
Office of Sponsored Programs
Baltimore MD 21250

Sub Contractor Numbers (c):

Patent Clause Number (d-1):

Patent Date (d-2):

Work Description (e): The subcontract supported the work of Dr. Kathleen Hoffman, the co-PI on the project.

Sub Contract Award Date (f-1): 7/1/2012 12:00:00AM

Sub Contract Est Completion Date(f-2): 3/1/2013 12:00:00AM

Inventions (DD882)

Scientific Progress

Technology Transfer

Final Report: Closing the Loop: Integrating Body, Muscle and Environment with Locomotion Central Pattern Generators

Tim Kiemel, Kathleen Hoffman

June 30, 2013

List of Figures

1 Statement of Problem

Animals move in response to threats from predators, a change in the environment, or to pursue prey. This motion is generated by a complex interaction of the neural circuits in the spinal cord and brain, the body, the muscles, sensory organs and the environment. Without sensory input, neural circuits are capable of producing movement by sending signals to motor circuits that in turn contract the muscles. Biomechanical systems of body, muscle and environment can also produce motion with simple activation input. However, in isolation, neither the neural circuit or the biomechanical system can produce movement efficient enough to support chasing prey or avoiding predators. Thus, it is essential that the neural circuit receive input from sensory organs that are affected by the position of the body, the activation of the muscle and the environment. Conversely, efficient movement also requires that the motor system receive signals from the neural circuit. Therefore, a central question in modeling integrated neuromechanical systems is how to close the loop between the neural circuit and the sensory feedback from the body, muscle, and environment. Understanding how these components interact at a systems level is important to understanding the complexities in vertebrate locomotion.

Vertebrate locomotion includes walking, swimming, and flying and each of these behaviors involves the interaction between the neural circuit, sensory organs, body, muscle, and environment. Each mode of locomotion has its own challenges and environments, but the feedback loop remains similar. We have closed the loop between the neural circuitry, body, and fluid environment for swimming locomotion, where the lamprey serves as a model system[1,2,3,4,5,6,7,8].

Our philosophy of modeling includes a hierarchy of models with varying degrees of detail and complexity. Certainly the computational power to simulate an all neuron simulation with

full muscle, body and fluids exists, yet the results may not yield insight into the mechanisms that comprise the system. Therefore, we have chosen to start with a tractable system in which the CPG is modeled with a phase model and the plant (body, muscle and fluid) is modified from McMillen et al.[9]. It is crucial to understand the closed loop feedback from the simple phase model perspective before incorporating more detailed realistic models for CPG or the fluid. Looking ahead to future research directions that would build on the work proposed here, the next step in the modeling hierarchy is to combine results with E.Tytell at JHU, who is using Floquet multiplier theory to understand which eigenmodes of the limit cycle are important to perturbations in the environment. Then, the combined work will be integrated into a two or three dimensional simulation of a Navier-Stokes fluid and elastic body[3].

2 Summary of results

We have taken two approaches to understanding the role of sensory feedback in locomotion: a control-theory approach and a CPG-based approach. In the control theory approach (§2.1), we have developed a general method of computing the optimal local feedback control law given a model of the plant (the mapping from muscle activation to movement) and a cost rate function that penalizes muscle activation and rewards speed through the environment. The first step in this method is to the compute the optimal steady-state swimming pattern, which we have done for a simple plant model of lamprey swimming (§2.2). In our CPG-based approach (§2.3), we have combined a simple CPG model with the plant model of §2.2 to produce a closed-loop model of lamprey swimming in which a the CPG produces a pattern of muscle activation which is modified by sensory feedback related to body curvature.

2.1 Computation of optimal feedback for the control of locomotion

We have a developed a general method of computing the optimal feedback control law for the control of periodic motion. Consider a locomotion control problem of the form

$$\begin{aligned} &\dot{x}(t) = f(x(t), u(t)), \\ &\text{cost rate } g(x(t), u(t)), \end{aligned}$$

where $x(t)$ is the state vector, $u(t)$ is the control vector, and $g(x, u)$ punishes the use of control (e.g., muscle activation) and rewards speed through the environment in the desired direction.

Let $\tilde{u}(t)$, $\tilde{x}_1(t)$, $\tilde{x}_2(t)$ be the open-loop periodic solution that minimizes the time average of $g(u(t), x(t))$. Let T be its period and $\hat{T} = T/2\pi$. Apply the change of coordinates in the vicinity of the limit cycle

$$\begin{aligned} x_1 &= \tilde{x}_1(\hat{T}\theta), \\ x_2 &= \tilde{x}_2(\hat{T}\theta) + r, \\ u &= \tilde{u}(\hat{T}\theta) + \hat{u}, \\ \hat{g}(\hat{x}, \hat{u}) &= g(h(\hat{x}, \hat{u})), \end{aligned}$$

where θ is absolute phase (mod 2π), r describes deviations in velocity, $\hat{u}$ describes deviations in the control signal, $\hat{x} = (r, \theta)$, and $(x, u) = h(\hat{x}, \hat{u})$ denotes the change of variables.

In the new variables $\hat{x}$ and $\hat{u}$, the system has the form

$$\begin{pmatrix} \dot{r} \\ \dot{\theta} \end{pmatrix} = \hat{f}(\hat{x}, \hat{u}) = \begin{pmatrix} A_{10}(\theta)r + A_{01}(\theta)\hat{u} + A_{20}(\theta)r^2 + A_{11}(\theta)r\hat{u} + A_{02}(\theta)\hat{u}^2 \\ \omega + B_{10}(\theta)r + B_{01}(\theta)\hat{u} + B_{20}(\theta)r^2 + B_{11}(\theta)r\hat{u} + B_{02}(\theta)\hat{u}^2 \end{pmatrix} + O(3),$$

$$\begin{aligned} \hat{g}(\hat{x}, \hat{u}) &= \hat{g}_{00}(\theta) + \hat{g}_{10}(\theta)r + \hat{g}_{01}(\theta)\hat{u} \\ &\quad + \hat{g}_{20}(\theta)r^2 + \hat{g}_{11}(\theta)r\hat{u} + \hat{g}_{02}(\theta)\hat{u}^2 + O(3), \end{aligned}$$

where $\omega = 1/\hat{T}$ and we have the subtracted the mean from $\hat{g}_{00}(\theta)$.

For any initial state $(r(0)), q(0))$, we want to choose $\hat{u}(t)$ for $0 \le t \le t_{\mathrm{f}}$, where t_{f} is a time far in the future, to minimize

$$V(r(0), \theta(0)) = D(\theta(t_{\mathrm{f}})) + \int_0^{t_{\mathrm{f}}} \hat{g}(r(t), \theta(t), \hat{u}(t))dt.$$

where

$$D(\theta) = -\frac{1}{\omega}\int_0^{\theta} \hat{g}_{00}(\phi)d\phi$$

so that V converges in the limit as $t_{\mathrm{f}} \to \infty$.

The solution is given by the Hamilton-Jacobi-Bellman (HJB) equation

$$0 = \min_{\hat{u}}[\hat{g}(r, \theta, \hat{u}) + \nabla V(r, \theta) \cdot \hat{f}(r, \theta, \hat{u})]$$

Using a perturbation analysis, we can approximate the solution of the HJB equation:

$$\begin{aligned} V(r, \theta) &= V_0(\theta) + V_1(\theta)r + r^{\mathrm{T}}V_2(\theta)r + O(||r||^3), \\ \hat{u} &= C_1(\theta)r + O(r^2), \end{aligned}$$

so that the solution of optimal feedback control problem in the vicinity of the limit cycle is

$$u = C_0(\theta) + C_1(\theta)r + O(r^2)$$

where $C_0(\theta) = \tilde{u}(\hat{T}\theta)$.

The quantity $F(r, \theta, \hat{u}) = \hat{g}(r, \theta, \hat{u}) + \nabla V(r, \theta) \cdot \hat{f}(r, \theta, \hat{u})$ to be minimized in the HJB equation can be written up to second order as

$$\begin{aligned} &F(r, \theta, \hat{u}) = F_{00}(\theta) + F_{10}(\theta)r + F_{01}(\theta)\hat{u} + r^{\mathrm{T}}F_{20}(\theta)r + r^{\mathrm{T}}F_{11}(\theta)\hat{u} + \hat{u}^{\mathrm{T}}F_{02}(\theta)\hat{u} \\ &= \hat{g}_{00}(\theta) + \hat{g}_{10}(\theta)r + \hat{g}_{01}(\theta)\hat{u} + r^{\mathrm{T}}\hat{g}_{20}(\theta)r + r^{\mathrm{T}}\hat{g}_{11}(\theta)\hat{u} + \hat{u}^{\mathrm{T}}\hat{g}_{02}(\theta)\hat{u} \\ &+ (V_1(\theta) + 2r^{\mathrm{T}}V_2(\theta))(A_{10}(\theta)r + A_{01}(\theta)\hat{u} + A_{20}(\theta)[r, r] + A_{11}(\theta)[r, \hat{u}] + A_{02}(\theta)[\hat{u}, \hat{u}]) \\ &+ (V_0'(\theta) + r^{\mathrm{T}}V_1'(\theta)^{\mathrm{T}} + r^{\mathrm{T}}V_2'(\theta)r) \\ &\quad (\omega + B_{10}(\theta)r + B_{01}(\theta)\hat{u} + r^{\mathrm{T}}B_{20}(\theta)r + r^{\mathrm{T}}B_{11}(\theta)\hat{u} + \hat{u}^{\mathrm{T}}B_{02}(\theta)\hat{u}), \end{aligned}$$

where

$$\begin{aligned}
F_{00}(\theta) &= \hat{g}_{00}(\theta) + \omega V_0'(\theta), \\
F_{10}(\theta) &= \hat{g}_{10}(\theta) + V_1(\theta)A_{10}(\theta) + V_0'(\theta)B_{10}(\theta) + \omega V_1'(\theta), \\
F_{01}(\theta) &= \hat{g}_{01}(\theta) + V_1(\theta)A_{01}(\theta) + V_0'(\theta)B_{01}(\theta), \\
F_{20}(\theta) &= \hat{g}_{20}(\theta) + (V_1 \circ A_{20})(\theta) + 2V_2(\theta)A_{10}(\theta) + V_0'(\theta)B_{20}(\theta) + V_1'(\theta)^{\mathrm{T}}B_{10}(\theta) + wV_2'(\theta), \\
F_{11}(\theta) &= \hat{g}_{11}(\theta) + (V_1 \circ A_{11})(\theta) + 2V_2(\theta)A_{01}(\theta) + V_0'(\theta)B_{11}(\theta) + V_1'(\theta)^{\mathrm{T}}B_{01}(\theta), \quad (1) \\
F_{02}(\theta) &= \hat{g}_{02}(\theta) + (V_1 \circ A_{02})(\theta) + V_0'(\theta)B_{02}(\theta). \quad (2)
\end{aligned}$$

To find the $\hat{u}$ that minimizes $F(r, \theta, \hat{u})$ for each r and $\hat{u}$, we solve

$$0 = \nabla_{\hat{u}} F(r, \theta, \hat{u}) = F_{01}(\theta)^{\mathrm{T}} + F_{11}(\theta)^{\mathrm{T}} r + 2F_{02}(\theta)\hat{u}$$

for $\hat{u}$. For $r = 0$, the solution must be $\hat{u} = 0$, since this corresponds to the solution of the open-loop optimal-control problem. Therefore, $F_{01}(\theta) = 0$. Then the solution to (2.1) is

$$\hat{u} = -\tfrac{1}{2}F_{02}(\theta)^{-1}F_{11}(\theta)^{\mathrm{T}} r. \quad (3)$$

Therefore,

$$\begin{aligned}
\min_{\hat{u}} F(r, \theta, \hat{u}) &= F_{00}(\theta) + F_{10}(\theta)r + r^{\mathrm{T}}F_{20}(\theta)r - \tfrac{1}{2}r^{\mathrm{T}}F_{11}(\theta)F_{02}(\theta)^{-1}F_{11}(\theta)^{\mathrm{T}}r \\
&\quad + \tfrac{1}{4}r^{\mathrm{T}}F_{11}(\theta)F_{02}(\theta)^{-1}F_{11}(\theta)^{\mathrm{T}}r \\
&= F_{00}(\theta) + F_{10}(\theta)r + r^{\mathrm{T}}\left(F_{20}(\theta) - \tfrac{1}{4}F_{11}(\theta)F_{02}(\theta)^{-1}F_{11}(\theta)^{\mathrm{T}}\right) r.
\end{aligned}$$

To solve the HJB equation, we want this minimum to be 0 for all r and θ. Therefore,

$$\begin{aligned}
F_{00}(\theta) &= 0, \\
F_{10}(\theta) &= 0, \\
F_{20}(\theta) - \tfrac{1}{4}F_{11}(\theta)F_{02}(\theta)^{-1}F_{11}(\theta)^{\mathrm{T}} &= 0.
\end{aligned}$$

We write $F_{20}(\theta)$ and $F_{11}(\theta)$ in the form

$$\begin{aligned}
F_{20}(\theta) &= G_{20}(\theta) + 2V_2(\theta)A_{10}(\theta) + wV_2'(\theta), \\
F_{11}(\theta) &= G_{11}(\theta) + 2V_2(\theta)A_{01}(\theta),
\end{aligned}$$

where

$$\begin{aligned}
G_{20}(\theta) &= \hat{g}_{20}(\theta) + (V_1 \circ A_{20})(\theta) + V_0'(\theta)B_{20}(\theta) + V_1'(\theta)B_{10}(\theta), \\
G_{11}(\theta) &= \hat{g}_{11}(\theta) + (V_1 \circ A_{11})(\theta) + V_0'(\theta)B_{11}(\theta) + V_1'(\theta)B_{01}(\theta).
\end{aligned}$$

Then $V_2(\theta)$ is the solution to

$$\begin{aligned}
&G_{20}(\theta) + 2V_2(\theta)A_{10}(\theta) + wV_2'(\theta) \\
&\qquad - \tfrac{1}{4}[G_{11}(\theta) + 2V_2(\theta)A_{01}(\theta)]F_{02}(\theta)^{-1}[G_{11}(\theta) + 2V_2(\theta)A_{01}(\theta)]^{\mathrm{T}} = 0.
\end{aligned}$$

Once we have solved for $V_0(\theta)$, $V_1(\theta)$ and $V_2(\theta)$, we can use (1) and (2) to solve for $F_{11}(\theta)$ and $F_{02}(\theta)$ and then use (3) to obtain the optimal feedback control law in the vicinity of the limit cycle.

2.2 Computation of optimal steady-state swimming for a simple model of lamprey swimming

To apply the method of §2.1 to a plant model of lamprey swimming, the first step is to find the optimal steady-state swimming solution. We have done this for a simple model of lamprey swimming, as described in this subsection. (We are currently in the process of implementing the feedback step of the method of §2.1 for this model.)

The plant model we used is based on Ekeberg (1993)[1] and McMillen & Holmes (2006)[9] with further simplifications. The body is modeled as a chain of n segments with $n-1$ links. For simplicity, we assume that all segments are identical (in contrast to the lamprey body which tapers from head to tail). The system has $n+2$ mechanical degrees of freedom: the 2-d position of the head and the angles of each of the n segments. Therefore, the state is described by a vector $x(t)$ of dimension $2n+4$. We assume that when a segment moves through the water there are resistive water forces in the directions perpendicular and parallel to the segment's orientation that depend on the segment's velocity components in these two directions.

We assume that the control vector $u(t)$ consists of the torques produced by muscles at each of the $n-1$ links. Therefore, we have a plant model of the form

$$\dot{x}(t) = f(x(t), u(t)),$$

where $x(t)$ has dimension $2n+4$ and $u(t)$ has dimension $n-1$.

We assume a simple cost rate that penalizes mean squared muscles torques and rewards velocity of the center of mass $v_{\mathrm{COM}}(t)$ in the leftward direction:

$$\text{cost rate } g(x(t), u(t)) = \frac{1}{n-1} \sum_{j=1}^{n-1} u_j(t)^2 - c v_{\mathrm{COM}}(t),$$

where the parameter c specifies the relative importance of swimming fast versus minimizing muscle activation.

To optimize steady-state swimming we minimize the average cost rate over one cycle of swimming by adjusting the following set of $6n-2$ parameters: the swimming frequency $f_{\mathrm{s}} = 1/T$; the initial 2-d velocity of the head and time derivative of the first segment angle; and the Fourier coefficients for modes 1, 3 and 5 describing link angles as a function of time. We assume left-right spatio-temporal symmetry, so we only need the odd-numbered modes. We assume that that at $t = 0$, the 2-d head position and first segment angle are zero. We have the equality constraints that the 2-d velocity of the head and time derivative of the first segment angle must be the same at the beginning and end of the cycle. To reduce the number of parameters, here we set the number of links n to be 6. We solve the constrained optimization problem using the Lagrange method as implemented by the `fmincon` function in Matlab. The average cost rate is computed by numerically integrating the plant system of ODEs over one cycle.

Figure 1 shows results of optimizing swimming for different rewards c for swimming speed. As the reward c increases, the lamprey swims faster (Fig. 1A). As in the lamprey, as swimming speed in the model increases, swimming frequency increases (Fig. 1B) and phase lags among muscle torques and body curvature at different locations along the body remain

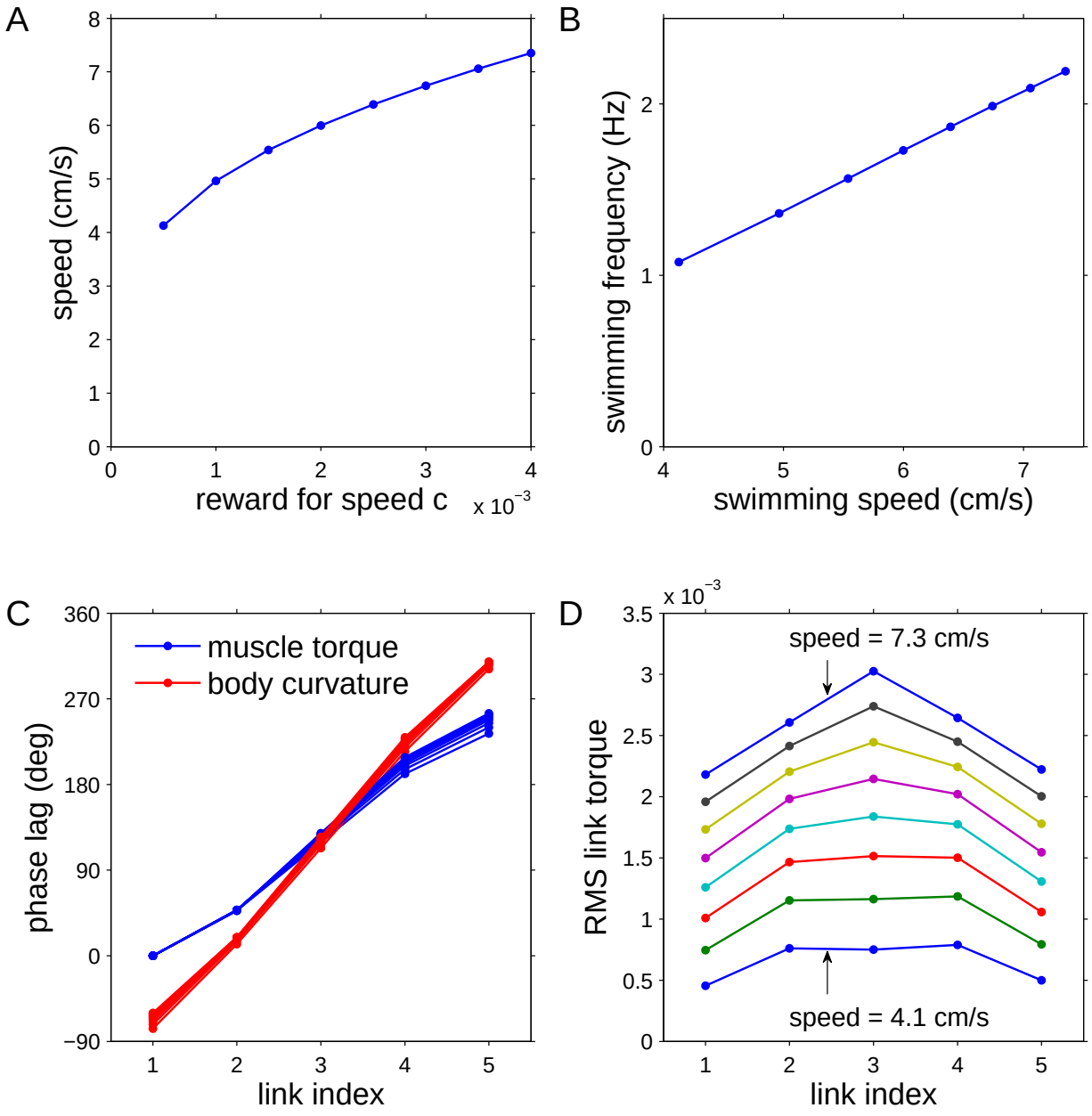

Figure 1: Optimal steady-state swimming as the reward for swimming speed is varied.

roughly constant (Fig. 1C). Also note that as in the lamprey, the wave of muscle activity moves more faster along the body than the wave of body curvature. As expected muscle torques also increase with increasing swimming speed (Fig. 1D).

2.3 A closed-loop CPG-based model of lamprey swimming

In this subsection we describe our CPG-based approach to understanding closed-loop locomtion. Vertebrate locomotion central pattern generators (CPG) are known to produce an electrical signal that is projected to the motorneurons, which in turn contract the muscle and propel the animal through the environment. Sensory input to the vertebrate locomotion CPG is known to modulate the signal of the CPG. In the model system that we are studying, the lamprey have several forms of sensory inputs. The lamprey lateral line system transmits information regarding the fluid flow around the body as a direct input through the lateral line nerve to the brain. Additionally, there are edge cells that sit on the margin of the spinal cord that transmit information directly to the locomotion CPG. Edge cells are stretch receptor, and essentially measure the curvature of the body. In our model of closed loop swimming, we focus on this type of sensory input and show that sensory input to the lamprey locomotion CPG modulate the motion of the animal though a closed feedback loop.

The vertebrate, and lamprey in particular, central pattern generator of locomotion is commonly represented by a chain of coupled oscillators with neural connections between the oscillators. Each individual oscillator can be represented by models with varying biological detail[6,10,1,8,11]. We consider the simplest model of a chain of n coupled phase oscillators:

$$\dot{\theta}_i \;=\; \omega + \sum_{j=1}^{n} \alpha_{i-j} \sin(\theta_j - \theta_i - \psi_{i-j}) + A_i \sin(\theta_i^{\mathtt{m}} - \theta_i - \psi_i^{\mathtt{m}}), \tag{4}$$

where θ_i for $i = 1, \ldots, n$ are the absolute phases (mod 2π) of oscillators in the chain ($i = 1$ for the oscillator nearest the head) and the parameter ω is the uncoupled angular frequency of the oscillators in the chain, which we assume to be the same for all oscillators, $\omega = 1Hz$.

Each oscillator in the central pattern generator receives two types of input. The first type of input, which we will call *internal inputs*, are from other oscillators in the central pattern generator. This describes the coupling between the oscillator in the locomotion CPG. The model assumes that coupling is *translation invariant*, meaning that the properties of the connection from oscillator j to oscillator i only depend on the relative position $k = i - j$: α_k is the strength of the connection and ψ_k is its preferred phase. Here, $k > 0$ for descending (toward the tail, or caudal) connections and $k < 0$ for ascending (toward the head, or rostral) connections. (Note the conflict between the anatomical terms "descending" and "ascending" and our indexing scheme in which i increases from head to tail.) There is no connection between an oscillator and itself, so $\alpha_0 = 0$. Supported by numerical evidence[12,13], we assume all-to-all coupling with coupling strength decaying exponentially with distance $|r|$: for $r > 0$ (descending connections), $\alpha_r = A_d e^{-|r|/\lambda_d}$; for $r < 0$ (ascending connections), $\alpha_r = A_a e^{-|r|/\lambda_a}$; for $r = 0$ (intrasegmental connections), $\alpha_r = 1$, where A_d, λ_d and A_a, λ_a are the amplitudes and length constants for descending and ascending connections, respectively. Experimental evidence suggests non-uniform coupling asymmetry, specifically, that short ascending connections are stronger than short descending connections, whereas long

descending connections are stronger than long ascending connections, which are reflected in the parameters A_d, λ_d and A_a, λ_a.

The second type of input into the central pattern generator is *external inputs* from the edge cells. This input provides the sensory feedback information into the central pattern generator. Experimentally, it has been shown that edge cells project directly onto the central pattern generator, and that it responds to both stretch and rate of stretch of the body, but the exact form of the feedback function has not been experimentally determined. We model the input from the edge cells using curvature information from the body equations. We tried two forms of feedback functions: one that was proportional to the body curvature, and one that was proportional to the square of the body curvature. We determined values of the constant of proportionality, which we will call the strength of feedback and denote by α_f, for which the animal reaches steady state swimming. The feedback function that was proportional to the body curvature produced unrealistic ranges of feedback strength that produced steady state swimming. The ranges in feedback strength to achieve steady state swimming were on the order of 10^{-6}, which essentially represents no feedback from the edge cells onto the central pattern generator. The feedback function that was proportional to the square of body curvature produced more realistic results in terms of values of feedback strength that produced steady state swimming, and these results are shown below.

For our simulations, we used a lamprey with ($n = 10$) segments, a Young's modulus of 0.7, and all-to-all coupling between the CPG oscillators with a slight non-uniform coupling asymmetry with $A_d = 10.0$ and $A_a = 10.1$. The simulation was performed in Matlab using the `ode23s` package. Figure 2a illustates the phase lags relative to the first oscillator for oscillators 2,4,6, and 8 of the body, in red, blue, green, cyan, respectively. The effect of the feedback is to slightly increase the phase lags between the oscillators, with oscillator 8 showing the largest increase, as expected since in incorportates the previous six increases. Figure 2b shows that the period is constant, as a function of body position, as expected in steady state swimming, but the period is different for each value of the feedback strength. In particular, the period decreases as the feedback strength increases. Figure 2c shows the maximum curvature as a function of body position for varying values of the feedback strength. As the feedback strength increases, the maximum curvature decreases for each body position, although the difference between the maximum curvatures at points along the body for a given feedback strength seems to increase as feedback strength increases. The final graph, figure 2d shows swimming speed as a function of feedback strength. There is a sharp rise in swimming speed for small feedback strength. The sharp increase is followed by a gradual decrease in swimming speed as feedback strength increases. We note here that swimming speeds on the order of 10–40 cm/sec are not realistic for a swimming lamprey, which may indicate that the feedback function is more complicated than simply squared curvature.

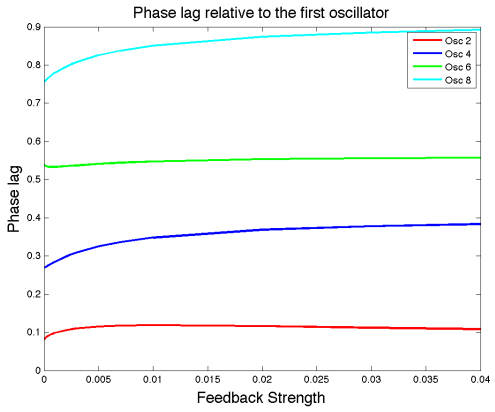

(a) Phaselags Relative to the first Oscillator

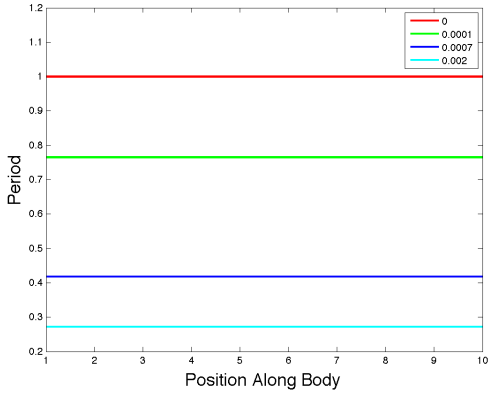

(b) Period

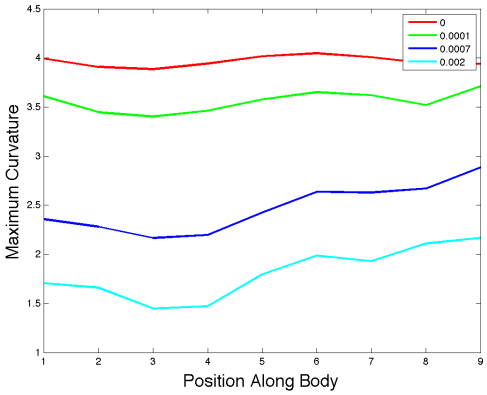

(c) Curvature

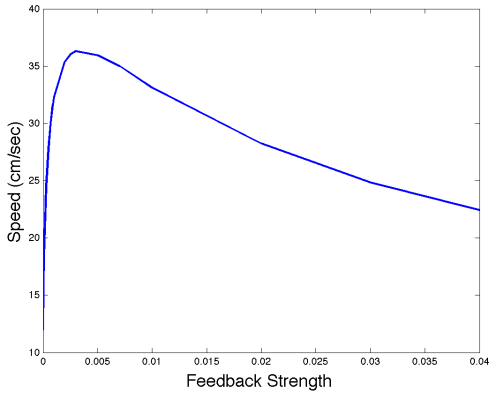

(d) Swimming Speed

Figure 2: Closed-loop swimming for various levels of feedback. This figure illustrates the effect of feedback on phase lags relative to the first oscillator in figure 2a, period in figure 2b, the curvature as a function of body position in figure 2c and velocity of swimming in figure 2d. In figure 2a, the phaselags relative to the first oscillator are shown as a function of feedback strength α_f, in a range of values that produce steady state swimming. Relative phaselags are shown for oscillator 2 in red, oscillator 4 in blue, oscillator 6 in green and oscillator 8 in cyan. Figure 2b shows that the period is a constant function of body position, as expected in steady state swimming, but that period decreases as feedback strength increases. Figure 2c plots maximum curvature as a function of body positions for varying values of feedback strength. The body curvature decreases as a function of feedback strength. The final graph figure 2d shows the effect of feedback strength on swimming speed.

Bibliography

1. Ekeberg, O. *Biol. Cybern.* **69**, 363–374 (1993).
2. T. McMillen, T. W. and Holmes, P. *PLoS Computational Biology* **4**(8) (2008).
3. Tytell, E., Hsu, C.-Y., T.Williams, Cohen, A., and Fauci, L. *PNAS* **107**, 19832–19837 (2010).
4. Prisco, G. V. D., Wallen, P., and Grillner, S. *Brain Res.* **530**, 161–166 (1990).
5. Buchanan, J. *Biol. Cybern.* **66**, 367–374 (1992).
6. Cohen, A., Holmes, P., and Rand, R. *J. Exp. Biol.* **116**, 3 (1982).
7. Cohen, A., Rossignol, S., and (Eds), S. G. *Neural Control of Rhythmic Movements in Vertebrates*. Wiley, (1988).
8. Ekeberg, O. and Grillner, S. *Phil. Trans. Roy. Soc. of London B* **354**(1385), 895–902 (1999).
9. McMillen, T. and Holmes, P. *J. Math. Biol.* **53**, 843–866 (2006).
10. Cohen, A., Ermentrout, G., Kiemel, T., Kopell, N., Sigvardt, K., and Williams, T. *Trends in Neurosci.* **15**, 434–438 (1992).
11. Kopell, N., Ermentrout, G., and Williams, T. *SIAM J. Appl. Math.* **51**, 1397–1417 (1991).
12. McClellan, A.D.and Hagevik, A. *Exp. Brain Res.* **126**, 93–108 (1999).
13. Miller, W. and Sigvardt, K. *J. Neurophys.* **83**, 465–476 (2000).